

Abu Attiffel Field: Gas Injection Process to Improve the Final Oil Recovery

Emilio Causin, Elio Rossi, Francesco Radaelli* and Ibrahim S. El Ageli**

عملية حقن الغاز لتحسين المسترد النهائي للنفط بحقل أبو الطفل

أميليو كوزين، وإليو روسي، وفرانسيسكو راديللي، وإبراهيم س. العجيلى

تم اكتشاف حقل أبو الطفل النفطي، العملاق بحوض سرت الرسوبي بالصحراء الليبية من قبل شركة آجيب عام 1967، حيث يتم إنتاج نفط من النوع الخفيف (41 درجة حسب مقاييس معهد البترول الأمريكي) من صخور الحجر الرملي القاري عند عمق يصل في المتوسط إلى حوالي 4200 متر تحت مستوى سطح البحر (13,800 قدم). بدأت عملية حقن الماء بعد سنتين من الإنتاج الأولى للنفط وشمل هذا حفر تسعه (9) آبار للمحافظة على الضغط. يبلغ معدل الإنتاج الحالي للنفط حوالي 91,000 برميل يومياً (314,500 م3) وبنسبة مياه تناهز 37% ويتوقع أن تكون نسبة المسترد النهائي حوالي 50%.

ونظراً لزيادة نسبة الماء مع النفط بشكل كبير في السنوات الأخيرة، فقد تم تقييم أسلوب الاسترداد الإضافي بهدف زيادة المسترد النهائي من النفط.

و ضمن عمليات الاسترداد الإضافي المأولة يعتبر حقن الغاز ملائماً لظروف المكمن بحقل أبو الطفل. أجريت معملياً دراسة أداء غازين مختلفين (ثاني أكسيد الكربون وغاز الفاصل) عند درجة حرارة المكمن وهي 145 درجة مئوية (292 درجة فهرنهايتية) وتحت ضغط 47.6 ميغا باسكال (6897 رطل على البوصة المربعة) وتم الحصول على إمتزاجية ثاني أكسيد الكربون (والتي تكفل أفضل الظروف لتحسين المسترد النهائي للنفط) مع زيت المكمن وتحت ضغط أقل من ضغط المكمن الأصلي إلا أن التجارب المعملية أوضحت حدوث ترببات بارافينية وتأكل في جميع الإختبارات.

وبالإضافة إلى ما يسببه الغاز الخفيف من ترببات بارافينية في الوسط المسامي ومشاكل التأكل فإنه لم يتمزج مع زيت المكمن عند ظروف المكمن الحالية.

ولقد تم تحقيق تحسن كبير في أداء الغاز الخفيف بإذابة حجم من غاز البترول المسال به وهو ما سمح بالحصول على الإمتزاجية عند ظروف المكمن الحالية (ألف قدم مكعب من الغاز الخفيف مشبع بحوالي 52 برميل من غاز البترول المسال). ومن أجل تأكيد كفاءة الإزاحة المجهري للنفط، تم إجراء عدة تجارب باستخدام غاز معزز عند ظروف المكمن الحالية. كما تم اختيار عينات لبية مماثلة لتكوين المكمن باستعمال تحاليل جهاز تصوير الرنين المغناطيسي النووي. كذلك تمتمحاكاة ثلاثة ظروف مكمنية (تشبع الزيت المتبقى، تشبع الزيت المتوسط، وتشبع الماء المستعصي).

وقد برهنت معظم التجارب كفاءة عالية جداً للإزاحة بالغاز المعزز الذي يتعلق بالمسترد النهائي بينما لعب نسيج الصخر دوراً مهماً عندما درست عينات عند درجة التشبع بالزيت المتبقى.

وأكّدت النتائج بأن الغاز المعزز كان أكثر كفاءة من الماء في المسترد النفطي النهائي على مستوى العينات الليبية.

* ENI – Agip Division.

** Agip Oil (Libyan Branch).

Abstract: The Abu Attiffel oilfield was discovered by Agip in 1967. This field is a giant reservoir located in the Sirt Basin of the Libyan desert. It is producing a volatile oil (41° API) from sandstones of continental environment at an average depth of 4,200 m b.s.l. (13,800 feet).

Water injection process started after two years of primary oil production, involving 9 injector wells for pressure maintenance purposes. Current field (main area) oil production rate is 91,000 BOPD (14,500 m³) with a water cut-off of about 37%. The final oil recovery is expected to be around 50%.

Since the water cut-off has dramatically increased in the last years, an EOR approach was evaluated in order to enhance the final oil recovery.

Among the conventional EOR processes, only gas injection was suitable for Abu Attiffel field because of its very severe reservoir conditions.

The performance of two different gases (CO₂ and separator gas) was studied in the laboratory at the average reservoir temperature of 145 °C (292 °F) and pressure of 47.6 MPa (6,897 psia).

CO₂ achieved miscibility (which assures the best conditions for an improvement of the final oil recovery) with the reservoir oil below the original reservoir pressure but paraffinic precipitation and corrosion phenomena occurred in all the tests performed.

Lean gas, besides causing paraffinic deposition in the porous media and corrosion problems, was not miscible with the oil under the current reservoir conditions.

A significant improvement of the lean gas performance was achieved by solubilizing a volume of LPG (liquefied petroleum gas) which permitted the miscibility to be reached under the current reservoir conditions (i.e. one MScf of lean gas enriched with about 52 bbl of LPG).

In order to confirm the improvement of the microscopic efficiency of the oil displacement, several experiments were carried out using enriched gas under current reservoir conditions.

Core plugs representative of the reservoir formation were selected on the basis of Nuclear Magnetic Resonance Imaging analysis.

Three different reservoir conditions (residual oil saturation, intermediate oil saturation and irreducible water saturation) were simulated.

Most of the tests demonstrated the very high displacement efficiency of the enriched gas as

regards final oil recovery. Gravitational forces slightly influenced oil recovery, while an important role was played by rock texture when samples at residual oil saturation were considered.

The results confirmed that the enriched gas was more effective than water in the final oil recovery at core scale.

INTRODUCTION

Abu Attiffel field is located in the Sirt Basin, about 400 km SE of Benghazi. It was discovered in 1967 and went on stream in 1972. The present oil rate (91,000 BOPD) is steadily decreasing from an average plateau of 150,000 BOPD maintained until 1993. A peak of 170,000 BOPD was recorded in 1990-92 after an infill drilling campaign. Up to now the cumulative oil production amounts to some 37% of the original oil in place (OOIP), and the expected final recovery is estimated at about 50%.

A water injection project started in 1974 with 9 injectors^[1,2] for pressure maintenance purpose. A daily rate of 350,000 bbl of water is presently injected and the field water cut has already reached 37%.

The rate decline and mature status of the field led Agip Oil's management to investigate the feasibility of an Enhanced Oil Recovery project to improve the final oil recovery. The gas injection was the only process suitable under the reservoir conditions of Abu Attiffel field. Carbon dioxide, lean gas and enriched gas were tested with the aim of finding out the most efficient solvent, miscible with the oil at the current reservoir conditions. After the selection of the gas, its performance was evaluated using real core plugs of the reservoir in order to evaluate the "microscopic oil displacement efficiency", in comparison with water injection process.

RESERVOIR CHARACTERISTICS

The reservoir is a west to east elongated horst, approximately 17 km long and 2-4 km wide, limited on all sides by faults and with a low dip of 5° to the north. Its OOIP is estimated at some 620 Mm³.

The oil production comes from the Upper Nubian Sandstones, a formation of a Lower Cretaceous age whose depth goes from 3886 to 4336 m b.s.l.

The oil-bearing rock is a fine to coarse-grained sandstone with interbedded shale and shaly-siltstones; it ranges in net thickness from 75 to 250 m. The

porosity (8%-16%) is intergranular and was preserved at rather good value by a syntaxial siliceous cementation which reduced the effect of the compaction after the deposition. The horizontal permeability spans from a few md to more than 1000 md, and the k_v/k_h ratio ranges from 0.48 to 1.23. The initial water saturation, which correlates quite well with the local porosity, averages 16%.

At discovery, a bubble point variation with the depth was recognized, but the oil resulted undersaturated at the initial pressure (47.6 MPa) through all the field. The basic volumetric properties and an average composition are listed in Tables 1 and 2, respectively.

The stock-tank crude has a 41° API gravity, its base is paraffinic at high wax content (36.7%) with an upper pour point of 39°C.

Representative gas and oil samples for the study were collected at the separator of the well A-17 (perforated interval: 4,137-4,232 m). They were recombined according to a gas-oil ratio of 245 Sm³/m³ to obtain a system saturated at 40.5 MPa at 145°C, *i.e.* at the current field conditions. In fact, a partial reservoir voidage lowered the initial pressure below the original average bubble point.

SELECTION OF THE MOST SUITABLE GAS

Experimental Procedures: The effect of each selected gas, when contacting the reservoir oil, was investigated both at static and dynamic conditions^[3] (Fig. 1).

In the first case, the volumetric behavior of several gas/oil mixtures, representing a wide range of

Table 1. Volumetric characteristics of reservoir oil.

Reservoir temperature	145 °C
Reservoir pressure	47.57 MPa
Bubble point pressure	40.46 MPa
Data at reservoir pressure	
Solution gas (Rs)	393.5 Sm ³ /m ³
O.R.V.F. (Bo)	2.2623
Reservoir oil density	543 kg/m ³
Reservoir oil viscosity	0.21 mPa s
Data at bubble point pressure	
Solution gas (Rs)	393.5 Sm ³ /m ³
O.R.V.F. (Bo)	2.3264
Reservoir oil density	528 kg/m ³
Reservoir oil viscosity	0.17 mPa s

Table 2. Fluid compositions (% MOL).

Components	Reservoir oil	Lean gas	Liquefied petroleum gas	Enriched gas (LGR = 290.3 m ³ /MSm ³)
Nitrogen	0.47	0.62	0.01	0.58
Carbon dioxide	3.06	3.76	0.70	3.58
Hydrogen sulfide	-	-	-	-
Methane	61.97	79.51	5.41	75.28
Ethane	8.72	10.43	6.51	10.21
Propane	2.86	3.13	9.29	3.48
I-Butane	0.66	0.63	5.50	0.92
N-Butane	1.10	0.92	10.81	1.49
I-Pentane	0.58	0.29	7.34	0.69
N-Pentane	0.72	0.28	8.19	0.73
Hexanes	1.99	0.27	20.80	1.44
Heptanes	1.94	0.09	13.63	0.86
Octanes (plus)	1.90	0.07	7.00	0.47
Nonanes	1.21	-	2.87	0.16
Decanes	1.16	-	1.22	0.07
Undecanes	0.74	-	0.40	0.02
Dodecanes	0.70	-	0.19	0.01
Tridecanes plus	10.22	-	0.13	0.01

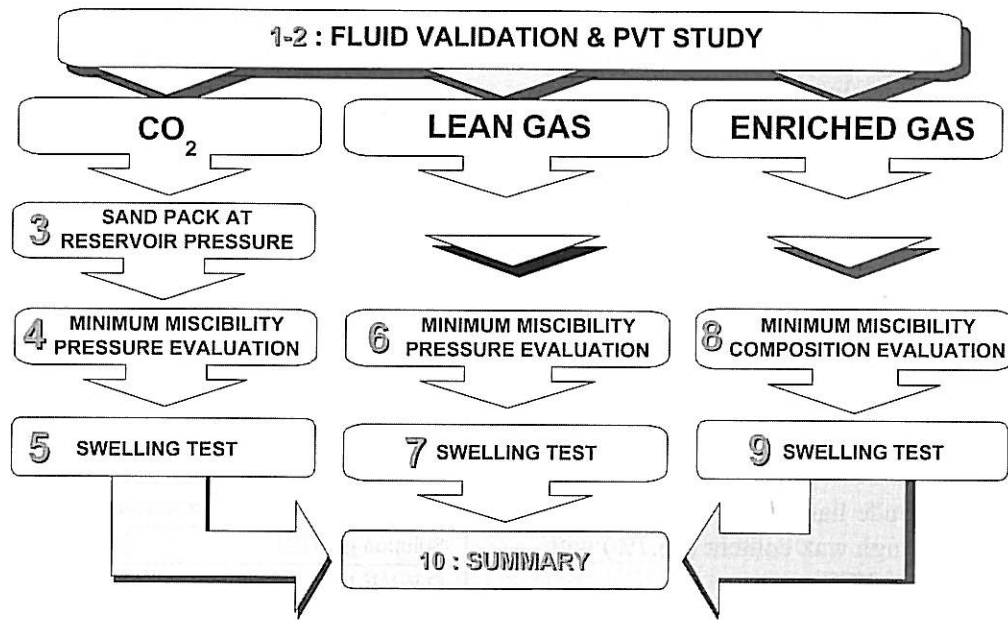


Fig. 1. Scheme of the phase 1 of the gas injection project.

different “injected gas-oil ratios” (IGOR, defined as the volume of gas – referred to standard conditions – added to a unit volume of reservoir oil at the original bubble point), was studied in a double windowed PVT cell. Each mixture was expanded at constant composition for measuring its saturation pressure and its “swelling factor”. This last parameter was defined as “the volume of the system at a given pressure divided by the volume of the reservoir oil at the original saturation pressure”. Furthermore, each system was identified as “oil” or “condensate”, according to the volumetric behavior observed when the pressure was lowered below the saturation point.

The dynamic experiments were performed in a slim tube equipment (Fig. 2), for finding out either the Minimum Miscibility Pressure (MMP)^[4] or the Minimum Miscibility Enrichment (MME)^[5]. The slim tube had a cross-sectional area of 38 mm² and a length of 18.23 m; the pore volume of the filling sand was 322 cm³ and the absolute permeability to air 3.95 μm^2 .

The rig consisted of two pumps for displacing either the stock-tank or the reservoir oil held in two high pressure vessels. In the thermostatic air bath were put:

- a high pressure bottle filled with gas;

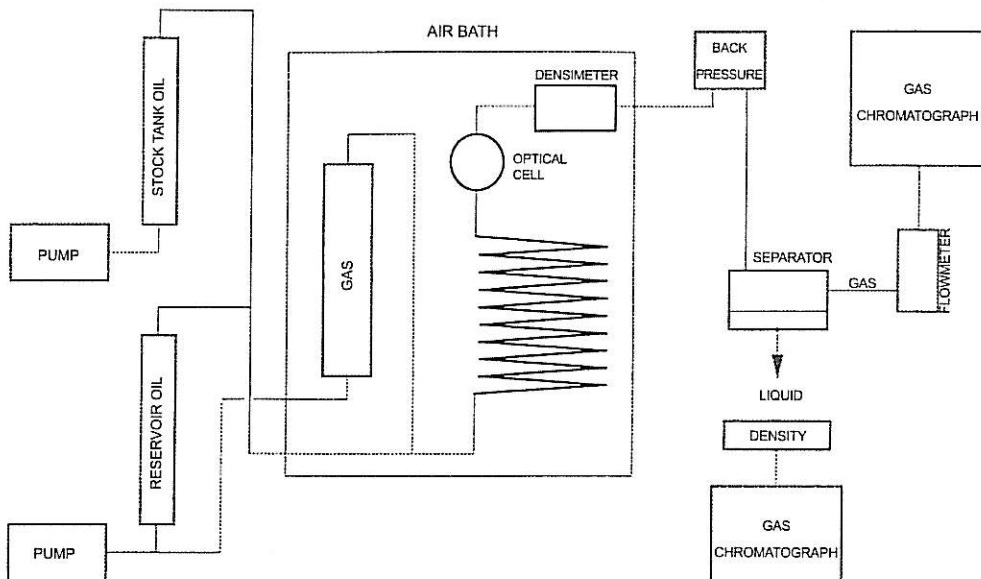


Fig. 2. Scheme of the oil displacement apparatus.

- the slim tube;
- a high pressure densimeter to measure the density of the produced fluid.

Gas and liquid phases were separated in a vessel, working at 15°C and atmospheric pressure. A mass-flowmeter continuously recorded the flow rate of the separated gas, whose chemical composition (up to C₈) was analysed every half an hour by a gas chromatograph set on line. The liquid samples were collected in glass bottles and weighed, as the high pour point of the crude did not allow any reliable volume measurements.

All the tests were carried out at a displacement velocity of 5.0 m/day (equivalent rate: 3.9 cm³/h), and at least 1.2 pore volume of gas was always injected during each experiment.

Phase Behavior of Oil/Carbon Dioxide Mixtures: Figure 3A shows the volumetric behavior of the reservoir oil swollen with CO₂ at different IGORs. The system behaved like an "oil" for IGOR up to 124.6 Sm³/m³ (corresponding saturation pressure: 42.9 MPa). Above it, for IGOR of 173.8 Sm³/m³ (corresponding saturation pressure: 43.8 MPa), the system appeared as a "condensate". The interval enclosed between these two values is the "critical point" zone, which was not investigated.

Five tests at 145°C and 53, 49.1, 42.9, 41.4 and 39.3 MPa were run to find out the MMP. The resulting value was very close to 42.9 MPa, as shown by the plot of the oil recovered (93.6, 93.0, 92.9, 88.2, 81.1% of OOIP, respectively) at CO₂ breakthrough vs. pressure (Fig. 4). For pressures beyond this value, the injectant and the oil develop a multicontact

miscibility, below it they are immiscible. The MMP found lies inside the transition zone between the "oil" and "condensate" systems outlined with the swelling tests.

It is quite interesting to notice that the CO₂ density (615-720 kg/m³) resulted always greater than that of the reservoir oil (530-540 kg/m³).

In the interval 41.4-49.1 MPa, *i.e.* around the MMP, the CO₂ stripping of the intermediate oil components destabilized the heavy paraffin fractions (C₂₅-C₆₀), and caused a wax precipitation.

At 42.9 MPa a drastic permeability reduction of the sand inside the slim tube was noticed, and the upstream section of the equipment became plugged. The appearance of a solid phase was also observed during the oil swelling tests.

Phase Behavior of Oil/Lean Gas Mixtures:

The composition of the lean gas, sampled at the Oil Centre, is listed in Table 2. Four tests at 145°C and 56.9, 53.0, 47.5 and 41.4 MPa were performed to determine the MMP. The oil recovered at lean gas breakthrough was 94.2, 93.4, 89.3 and 46.5% of OOIP, respectively. The plot of these data vs. pressure (Fig. 5) gave a MMP value of 48.1 MPa, which is higher even than the original reservoir pressure. The miscible process was identified as vaporizing gas drive^[6].

In the interval 47.5-41.4 MPa, well below the MMP, precipitation of heavy paraffins (C₃₀-C₆₀) was still observed. However, the phenomenon was less severe than that recorded during the CO₂ displacement. In fact, at 41.4 MPa the precipitated waxes caused a permeability reduction only in the

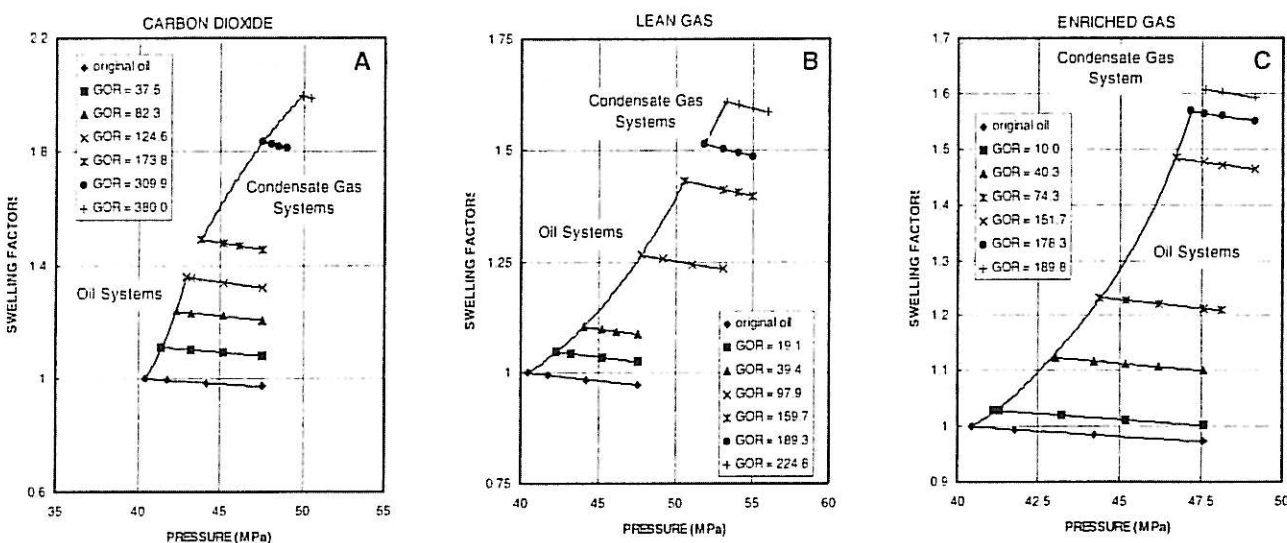


Fig. 3. Swelling factors of different gas/oil systems for several injection G.O.R.

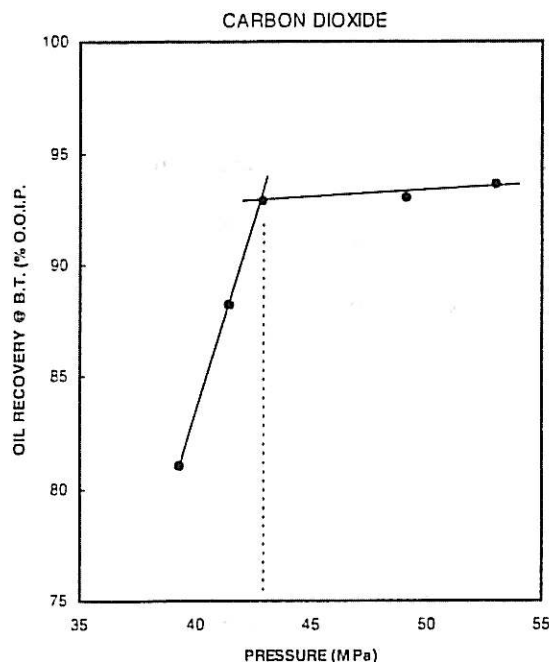


Fig. 4. MMP of carbon dioxide with Abu Attiffel oil.

inlet part of the slim tube and a partial plugging of the upstream section of the equipment.

The swelling tests (Fig. 3B) showed that the systems oil/lean gas behaved as "oil" up to an IGOR of $159.7 \text{ Sm}^3/\text{m}^3$ (corresponding saturation pressure: 50.6 MPa). Above it, for IGOR of $189.3 \text{ Sm}^3/\text{m}^3$ (corresponding saturation pressure: 51.9 MPa), the system appeared as "condensate".

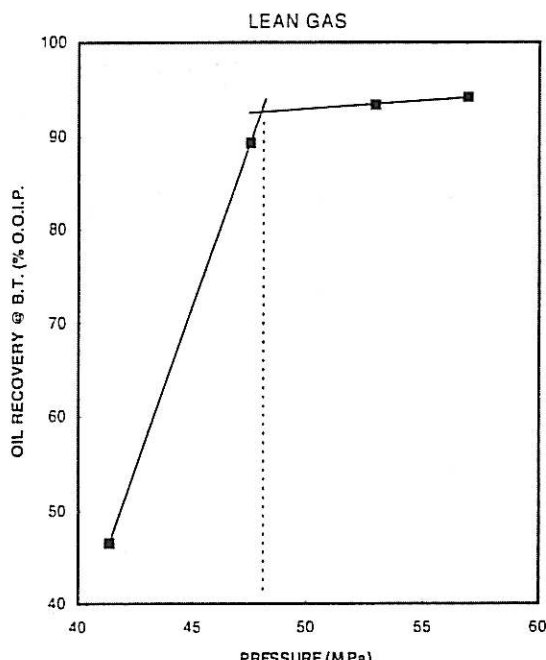


Fig. 5. MMP of lean gas with Abu Attiffel oil.

Lean Gas Enrichment with LPG: Because the lean gas miscibility was attained at too high pressure, it was decided to investigate to what extent it should be enriched with LPG(MME) to obtain a multicontact miscibility. The experiments were run with the equipment and according to the lab procedures employed during the MMP displacements, except the pressure was kept constant at 41.4 MPa to maintain the oil in single liquid phase. Four injectant mixtures, prepared according to different "liquid gas ratios" (LGR, defined as the LPG volume – referred at the sampling conditions 23°C , and 1.3 MPa – added to 10^6 Sm^3 of lean gas) were tested, namely 250, 710, 1000, 1670 m^3/MSm^3 .

The results of all these tests were compared with those of the lean gas displacement (LGR=0) performed at the same conditions. The trend analysis of the separated gas composition and the effluent density helped considerably the interpretation. For example, the oil displacement became "piston-like" passing from the lean gas to the richest injectant (LGR=1670 m^3/MSm^3) as shown by the trend of methane concentration in Fig. 6. The same conclusion is attainable also looking at the density (Fig. 7A), whose trend becomes more and more smooth as the injectant is enriched.

The most probable displacement mechanism was a condensing/vaporizing gas drive, with the condensing process prevailing as the gas was enriched^[6].

The MME was quantitatively evaluated plotting the oil recovered at gas breakthrough *vs.* LGR (Fig. 7B). It produced $290.3 \text{ m}^3/\text{MSm}^3$ at 145°C and 41.4 MPa (Fig. 7C). The injectant composition, measured after the LPG solubilization in a corresponding volume of lean gas, is presented in Table 2.

Phase Behavior of Oil/Enriched Gas Mixtures: Figure 3C shows the volumetric behavior of the reservoir oil swollen with enriched gas (LGR=290.3 m^3/MSm^3) at different IGORs. The transition zone between "oil" and "condensate" occurred only at high pressure. In fact, the system behaved like a liquid for IGORs up to $178.3 \text{ m}^3/\text{MSm}^3$ (corresponding saturation pressure: 47.2 MPa), and like a gas for an IGOR of $189.8 \text{ m}^3/\text{MSm}^3$ (corresponding saturation pressure: 47.6 MPa). The phase transition took place after a minimum change in the system composition, as proved in the following table which reports the chemical analysis of the two mixtures, compared with the original oil and MME gas compositions.

IGOR Sm ³ /m ³	Moles (%)									
	CO ₂	N ₂	C1	C2	C3	C4	C5	C6	C7	C8+
178.3	3.30	0.52	67.95	9.40	3.17	2.11	1.42	1.81	1.49	8.83
189.8	3.30	0.52	68.15	9.43	3.18	2.13	1.42	1.81	1.47	8.59
Original oil	3.06	0.47	61.97	8.72	2.86	1.76	1.30	1.99	1.94	15.93
MME gas	3.58	0.58	75.28	10.21	3.48	2.41	1.42	1.44	0.86	0.74

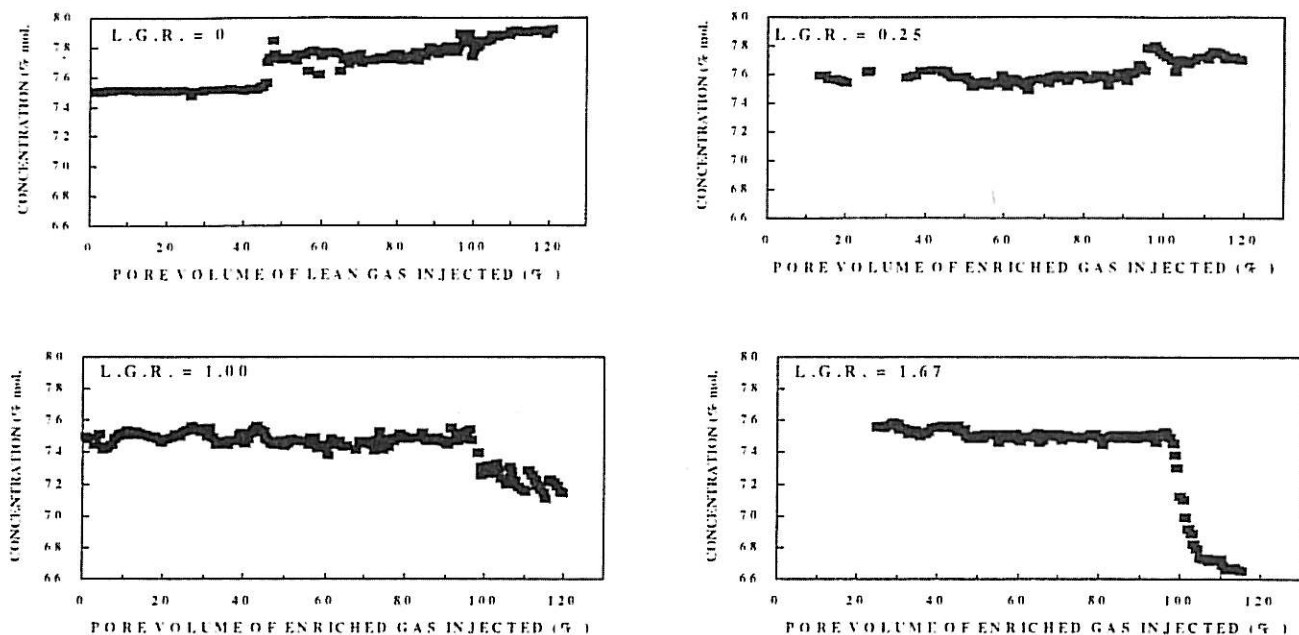


Fig. 6. Separator gas composition (methane concentration trend) for different L.G.R.

On the basis of these results, the enriched gas obtained vaporizing LPG in the lean gas was the most suitable under the current reservoir conditions. With an enrichment of 290.3 m³/MSm³ miscibility was attained by, condensing/vaporizing gas drive. Unlike the two other solvents, neither paraffin precipitation nor corrosion occurred in all the tests, therefore this injectant was retained for future field applications.

MICROSCOPIC OIL DISPLACEMENT EFFICIENCY

The experiments previously described had the aim of understanding gas-oil interactions. The effects of the reservoir rock texture and mineralogy, and the impact of water saturation on oil recovery were not taken into consideration.

A set of oil displacement tests was planned in order to determine the "microscopic oil displacement efficiency" of the enriched gas. As known^[7], the efficiency of a displacement process is quantified by

the oil recovery factor (E_R), which is defined as the ratio between the volume of oil produced and the volume of oil initially present in the reservoir rock. It depends on the volumetric invasion efficiency (E_V) and the displacement efficiency (E_D) or microscopic efficiency. The oil recovery factor is expressed as the product of macroscopic efficiency multiplied by microscopic efficiency. E_V is evaluated by numerical models, while E_D is determined at core scale using lab experiments described in the following section.

Selection of the Rock Samples: Since no core of the reservoir main area (Upper Nubian Sandstone) was available for this study, some cores of a peripheral well, which was recently drilled for another reason, were used.

A detailed petrographic and sedimentological study was performed in order to recognize the typical facies of the main reservoir area of the Abu Attifel field. The study showed that the less cemented samples tend to show the best permeability. Moreover, a pore network study enables us to conclude the following:

- 1) Samples with permeability over 100 md were

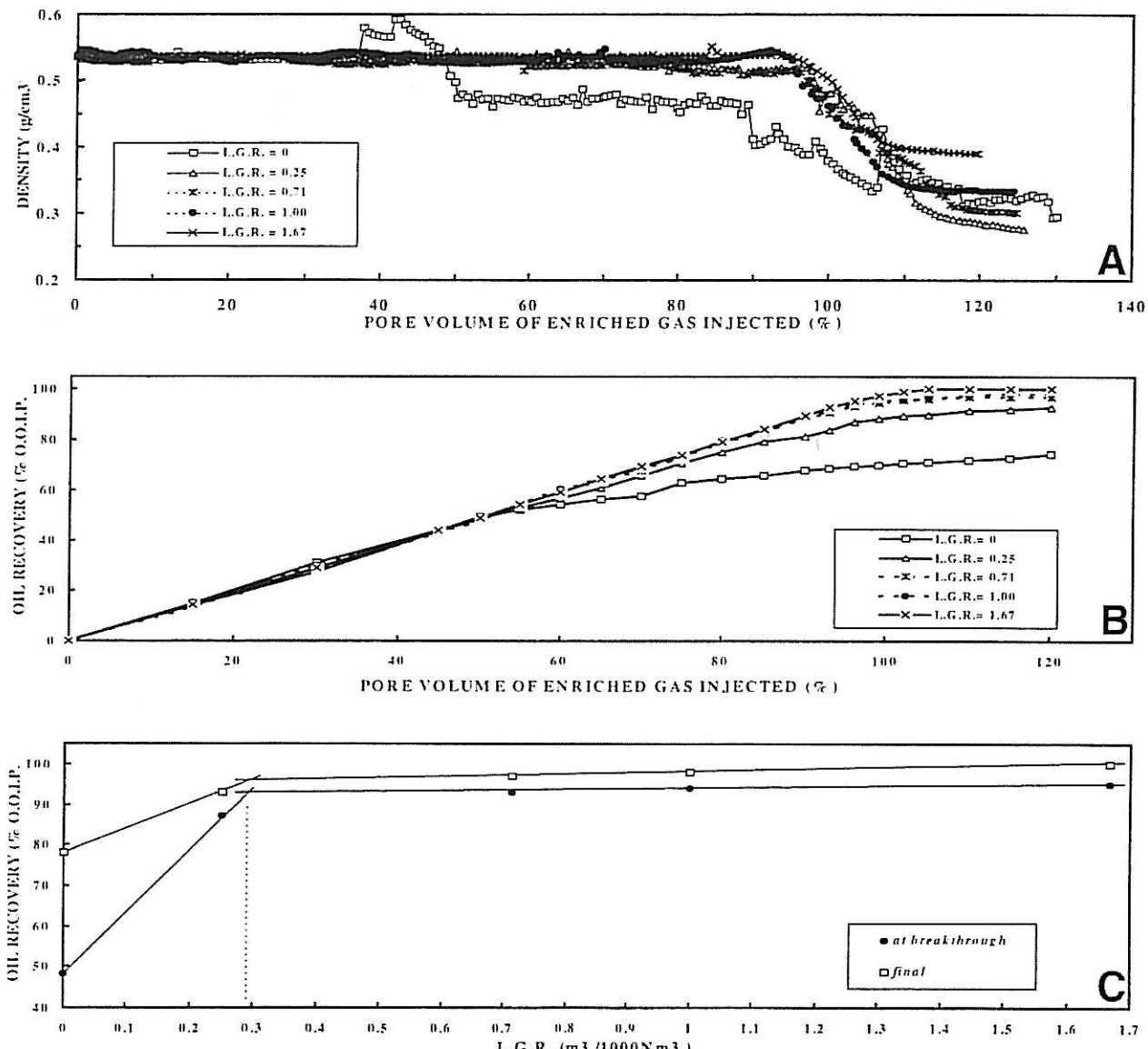


Fig. 7. Effluent density, oil recovery and M.M.E. determination.

characterized by well-connected, large primary pores and relatively high porosity, with a low content in total authigenes (quartz overgrowths, kaolinite and chlorite).

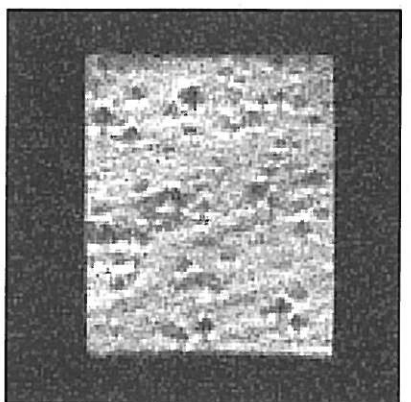
2) Samples with permeability ranging from 10 to 100 md were largely influenced by sedimentological features such as cross lamination. Along these features, stronger quartz cementation, more abundant pore-filling kaolinite and compaction-enhancing clay drapes were often observed; this deteriorates the pore structure which creates permeability barriers on a microscale.

Finally, a routine core analysis study was performed on plugs of 5 cm diameter and 5-6 cm length. After saturating the selected plugs with water, Nuclear Magnetic Resonance Imaging equipment

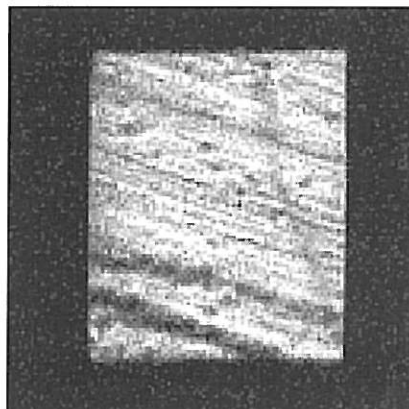
(MRI) was used to evaluate the type of heterogeneity of their internal texture and fluid distribution, without destroying them.

Analysis of the MRI images (the white zones of the images show the greatest water saturation. Water saturation decreases as the colour changes from white to black) highlighted four types of rock samples among the selected plugs:

- *Type 1. Homogeneous samples with subrounded non-porous zones.* The texture observed is probably due to cementation by patchy carbonates, commonly observed in Upper Nubian Sandstones; the other possibility is the presence of large-size quartz grains, but this is less likely, considering the normal grain-size of sandstone (Fig. 8).



Quartz+heavies	82 %
Feldsparts	0.5 %
Pseudo matrix	0.5 %
Quartz overgrowth occlusive	1.5 %
Quartz overgrowth part. occlusive	3 %
Carbonate occlusive	1 %
Chlorite	3 %
Kaolinite	8.5 %



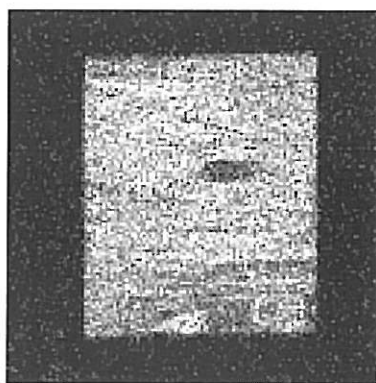
Quartz+heavies	77.5 %
Orthomatrix	1 %
Matrix rim	0.5 %
Quartz overgrowth occlusive	2 %
Quartz overgrowth part. occlusive	14.5 %
Kaolinite	4.5 %

Fig. 8. MRI images of rock type 1 and 2.

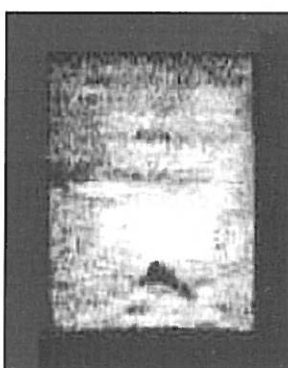
- *Type 2. Laminated samples.* The cross lamination, which is either well- developed or barely visible, is highlighted by more or less saturated laminae; this is due to a reduction in grainsize and the presence of depositional or diagenetic clays which produce a local permeability barrier. The presence of laminae with very low fluid saturation may be due to the preferential precipitation of carbonate cements along these laminae. This is also demonstrated by the precipitation of carbonate cements along these laminae. This is also demonstrated by the

occurrence of subrounded non-porous zones in the laminae (Fig. 8).

- *Type 3. Homogeneous sample.* Only faint depositional structures are present and saturation is fairly homogeneous. The dark, isolated, low-saturated structure is probably a clay clast (Fig. 9).
- *Type 4. Heterogeneous rock with crude lamination.* This type of sample is quite common at the basal part of fluvial cycles, where uniformity of grainsize, cementation and occurrence of clay clasts is at a maximum. High porosity zones with very large pores can be isolated into a relatively



Quartz+heavies	78 %
Quartz overgrowth occlusive	2.5 %
Quartz overgrowth part. occlusive	18.5 %
Kaolinite	1 %



Quartz+heavies	67.5 %
Orthomatrix	32.5 %

Fig. 9. MRI images of rock type 3 and 4.

less porous network with non-porous zones due to clay clasts or cementation (Fig. 9).

All the samples were water-wet.

OIL DISPLACEMENT TESTS

Experimental Procedure: All the oil displacements using water and enriched gas were carried out at a high pressure and high temperature rig shown in figure 10^[8]. The selected core plugs were washed and saturated with formation water (209 g/l salinity) and brought to irreducible water saturation conditions using a synthetic oil and centrifugation. After MRI analysis all the samples were mounted in a suitable high pressure and high temperature core-holder inserted in a thermostatic air bath. 5-10 pore volumes (PV) of recombined oil were pumped through the plug at a flow rate (which varied according to the petrophysical parameters of the sample) of 2.4-3.2 m/day in order to measure the oil permeability under residual water saturation (Swi).

All the displacements were carried out under a capillary regime^[9,10] in order to simulate the flow rate present in the bulk of the formation as accurately as possible under the current reservoir conditions. For the fluids being studied, interfacial tension and density values at reservoir temperature and at different pressures were experimentally determined. Table 3 shows the results obtained. In particular, the interfacial tension between water-oil, gas-water and gas-oil systems was determined using “pendant drop apparatus”^[11,12].

Water Injection: The oil recovery through water injection and water-oil relative permeability was determined following an unsteady state method, whereby water was injected (10-20 PV) at the same flow rate as recombined oil, and oil production and pressure drop at the core ends were recorded. The relative permeability values at the end points were directly calculated from experimental data. The

relative permeability curves were obtained using a calculation code based on an implicit method developed by Watson^[13].

Enriched Gas Injection: In the case of oil displacements using enriched gas, the following three different rock saturations were simulated:

- *Residual oil saturation (to simulate complete water-flooded zones).* To obtain these experimental conditions, the enriched gas was injected through samples which were previously flooded by water.
- *About 50% of oil saturation (to simulate zones under the current average oil saturation).* The plugs in Swi conditions were saturated with recombined oil. A known volume of water was injected in order to obtain the desired oil saturation. Finally, enriched gas was injected.
- *Irreducible water saturation (to simulate non-water-flooded zones).* To simulate these reservoir zones, the core plug brought to Swi conditions was saturated with recombined oil and then flooded with enriched gas.

RESULTS

Oil Displaced by Water: The scope of this step was to estimate residual oil saturation after the water-flooding process using more realistic conditions (reservoir conditions) than possible, when the conventional laboratory approach is adopted. The results of five tests are given in Table 4.

The lowest oil recovery, after the water-flooding process, of sample 41 (rock type 2) was due to its rock texture characterized by low permeability layers.

These results were compared with those obtained under laboratory conditions in previous petrophysical studies. As figure 11 shows, the final oil recovery obtained during tests under reservoir conditions was lower. The main conclusion drawn was that the efficiency of the water-flooding process under

Table 3. Interfacial tension between different systems.

Pressure (MPa)	Oil		Enriched gas		Interfacial tension (mN/m)		
	Density kg/m ³	Viscosity (mPa. s)	Density kg/m ³	Viscosity (mPa.s) ^(o)	Oil- water	Gas- water	Gas- oil
47.6	562.5	0.23	297.5	0.0386	24.0	32.3	<0.1 ^(o)
44.2	557.8	0.22	286.5	0.0367	25.2	33.4	<0.1
41.8	553.4	0.21	-	-	-	34.5	-
41.1	552.1	0.20	275.1	0.0349	27.0		<0.1

Table 4. Results of oil displaced by water.

Oil recovery									
Sam. no.	Pore Volume (ml)	Liquid perm. (md)	Swi (%)	Sor (%)	@Break-through (%)	Final (%)	Kro @Swi	Krw @Sor	Capillary number (Nc)
41	13.41	53	18.6	31.9	43.1	60.85	0.007	0.011	4.33×10^{-8}
170	15.78	37	10.4	16.6	66.5	81.43	0.4	0.39	3.67×10^{-8}
34	14.58	39	4.1	20.4	64.4	79.59	0.3	0.16	3.98×10^{-8}
37	15.37	18.3	16.6	19.9	39.0	76.62	0.062	0.042	3.78×10^{-8}
63.5	13.10	5.7	7.1	27.8	54.2	70.33	0.95	0.82	4.45×10^{-8}

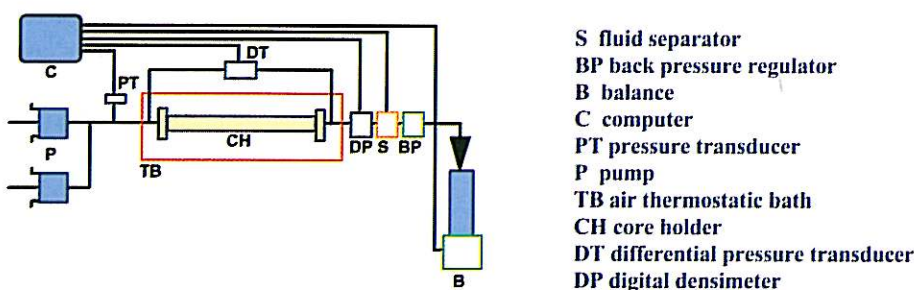


Fig. 10. Sketch of the experimental flooding rig.

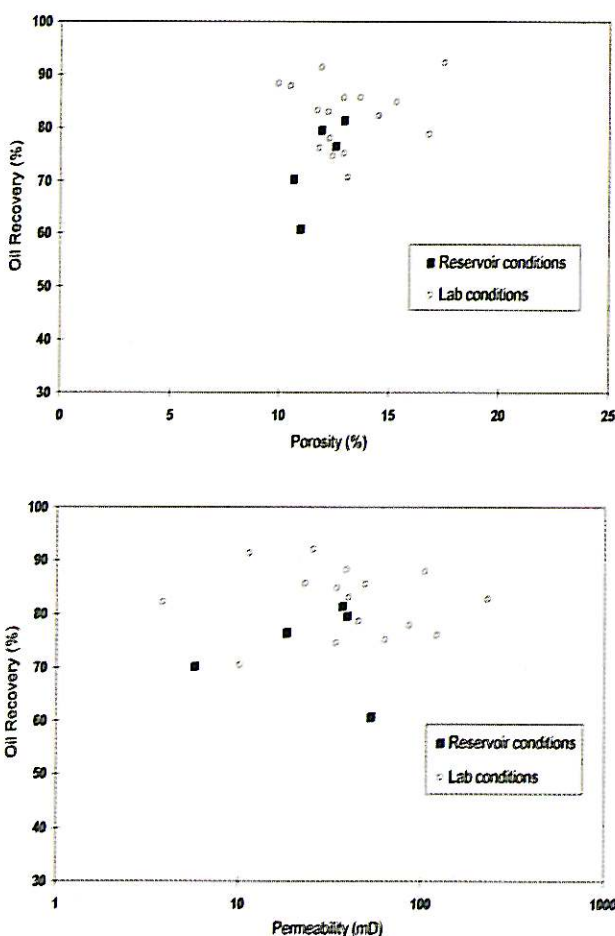


Fig. 11. Oil recovery by water-flooding vs. porosity and permeability.

reservoir conditions was poorer than that obtained following the conventional approach.

Oil Displaced by Enriched Gas: Four tests were carried out for each of the three different oil saturations which characterized the rock samples at the beginning of gas injection.

Samples under residual oil saturation. The main results obtained are summarized in Table 5. The following points characterized these oil displacements:

- the final oil recovery was achieved after the injection of less than 1.5 PV of enriched gas and its value was greater than 95% in samples with the lowest permeability;
- oil production began after significant water (mobile phase) production. Figure 12 shows an example where the cumulative fractions of oil and water produced are plotted together with the cumulative gas produced (associated and injected gasses);
- gas stripping of the oil intermediate components (C_{13} - C_{19}) took place in all the displacements;
- samples with greater liquid permeability had an early gas breakthrough with a consequent low oil recovery value (less than 75%);
- rock heterogeneity greatly influenced additional oil recovery; the most homogeneous samples gave the lowest oil recovery compared to other more heterogeneous ones, probably because the residual oil was spread over a larger rock volume;

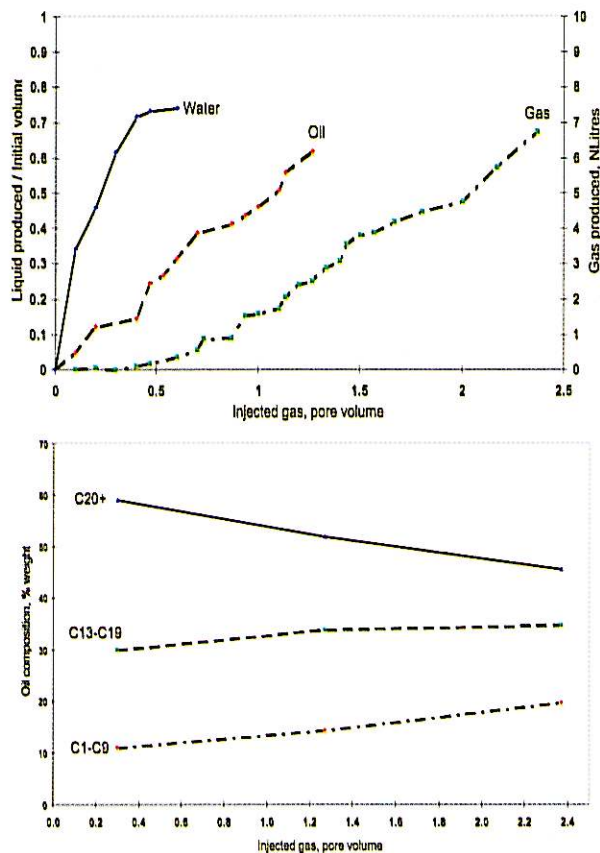


Fig. 12. Rock sample under residual oil saturation: oil displacement by gas, fluid production and composition of produced oil.

- the volume of enriched gas needed to cover a unit volume of reservoir ranged from 11,400 to 1,900 Nm^3/m^3 , which, at reservoir conditions, considering a deviation factor (z) of the gas of 1.0834, became 5.3-7.5 m^3/m^3 .

Samples under intermediate oil saturation. The oil displacement results are shown in Table 5. The following conclusions were drawn:

- final oil recovery ranged from 63 to 97% within a 1 PV of enriched gas injected;
- water production began before oil, probably because of a more favorable relative permeability of the gas-water system compared to gas-oil system (the rock was water-wet). Figure 13 shows an example where the cumulative fractions of oil and water produced are plotted together with the cumulative gas produced (associated and injected gasses).
- gas stripping of oil intermediate components took place in all displacements;
- the composition of the gas flashed from the oil produced showed an enrichment of light components (C_1 - C_9);
- two displacements, carried out on cores in vertical position, gave an incremental oil recovery which ranged from 3 to 8%;

Table 5. Oil recovery after the injection of the enriched gas.

Sample no.	Rock type	Porosity (%)	Liquid perm. (md)	Oil saturat. (%)	Gas volume		Final oil recovery
		@ Reservoir conditions	@ Reservoir conditions	@ Reservoir conditions	(Nm ³ /m ³)	@ Reservoir conditions	(% OIP)
Residual oil saturation (Sor)							
170	1	12.9	37.0	16.6	1944	7.44	74.43
63.5	1	10.6	6.0	27.6	1382	5.29	95.5
34	3	11.9	39.0	27.6	1743	6.67	61.7
37	2	12.5	18.0	21.5	1479	5.66	95.5
Intermediate oil saturation (So 50%)							
170	1	12.9	37.0	40.4	1036	3.96	63.1
70	2	11.6	31.0	51.2	466	1.78	95.3
68	2	12.8	7.0	51.7	457	1.75	88.5
151.8	2	12.4	16.0	49.1	565	2.16	96.9
68 Vert.	2	12.9	7.0	47.9	539	2.06	91.0
170 Vert.	1	11.6	37.0	46.8	922	3.53	68.4
Irreducible water saturation (Swi)							
32	4	10.9	30.0	88.5	482	1.84	94.1
100	2	12.7	15.0	93.5	349	1.34	98.0
66.5	1	10.4	33.0	82.8	474	1.81	99.1
193.5	1	12.6	55.0	93.5	288	1.10	99.0

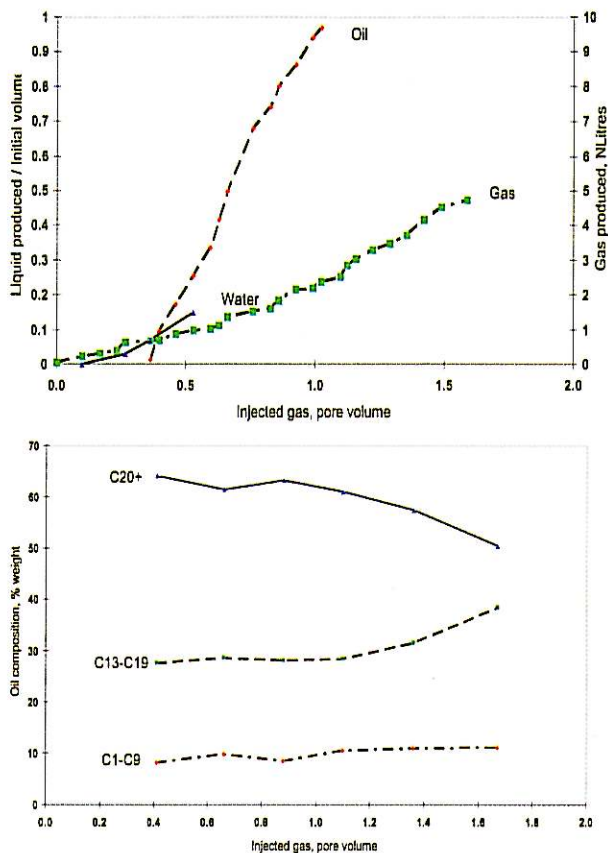


Fig. 13. Rock sample under intermediate oil saturation: oil displacement by gas. Fluid production and composition of produced oil.

- the volume of enriched gas needed to cover a unit volume of reservoir ranged from 450 to 1050 Nm³/m³, which, at reservoir conditions, considering a deviation factor (z) of the gas of 1.0834, became 1.70-4.0 m³/m³.

Samples under irreducible water saturation. The oil displacement results were shown in Table 5. The following conclusions were drawn:

- final oil recovery exceeded 94% in all the tests and is not greatly influenced by petrophysical parameters and rock texture. Figure 14 shows an example where the cumulative fraction of oil produced is plotted together with the cumulative gas produced (associated and injected gasses);
- gas stripping of oil intermediate components took place in all displacements;
- the composition of the gas flashed from the oil produced showed an enrichment of light components (C₁-C₉);
- the volume of enriched gas needed to cover a unit volume of reservoir ranged from 300 to 500 Nm³/m³, which, at reservoir conditions,

considering a deviation factor (z) of the gas of 1.0834, became 1.1-1.9 m³/m³.

The volume of enriched gas injected needed to recover a unit volume of reservoir oil was plotted against the oil saturation of the rock. In figure 15 the values with oil recovery greater than 90% have been highlighted. As one can see, the oil recovery values of rock samples with low oil saturation are greatly affected by rock heterogeneity. This means that, at field scale, the microscopic efficiency of oil displacement using enriched gas for well water-flooded zones (near Sor conditions) will be difficult to estimate, without good knowledge of the rock textures of these zones. For non-water-flooded zones, we can estimate that a 1 m³ of reservoir oil volume to be recovered will require less than 400 Nsm³/m³ of enriched gas with an E_D value greater than 90%.

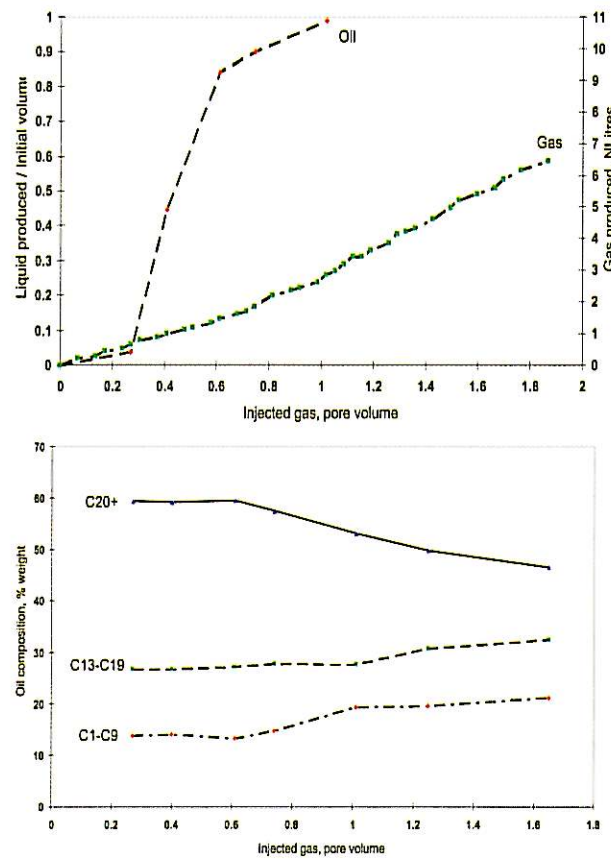


Fig. 14. Rock sample under irreducible water saturation: oil displacement by gas. Fluid production and composition of produced oil.

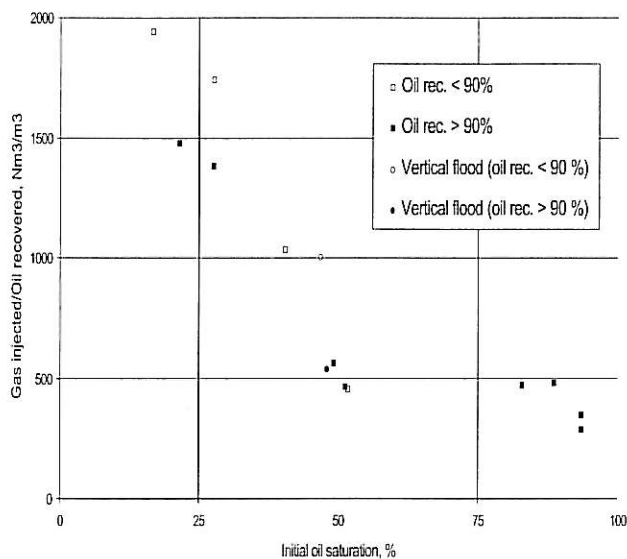


Fig. 15. Gas volume required to recover one cubic meter of reservoir oil at different oil saturations of the rock.

CONCLUSIONS

The behavior of three injectants, potentially available in the area, was investigated under Abu Attiffel reservoir conditions, namely:

Carbon Dioxide. It does not appear as the most suitable solvent for field applications. In fact, it developed miscibility, even though at a pressure level (42.9 MPa) a little higher than the current reservoir pressure (40.5 MPa), with precipitation of heavy paraffins noticed both during the displacements in slim tube and the swelling tests. Moreover, a large corrosion took place in some parts of the lab. equipment. The handling of these problems at field scale should affect considerably the operating costs.

Lean Gas. It is still an inadequate solvent because it becomes miscible only at 48.1 MPa, a pressure even higher than the original one (47.6 MPa). Moreover, paraffin precipitation and corrosion were again noticed during the experiments.

Enriched Gas. Obtained vaporizing LPG, available on the field, in the lean gas. With an enrichment of $290.3 \text{ m}^3/\text{Msm}^3$ miscibility was attained by condensing/vaporizing gas drive. Unlike the two other solvents, neither paraffin precipitation nor corrosion occurred in all the tests, therefore this injectant was retained for future field applications.

Most of the tests presented a very high oil recovery value, which means a high efficiency of oil displacements using enriched gas.

Owing to miscibility between oil and enriched gas, gravitational forces only partly influenced final oil recovery, whereas the rock's internal rock texture greatly influenced oil recovery when residual oil saturation conditions were reached in the formation. For higher oil saturations, the rock texture effect was far less evident.

The enriched gas volume needed to recover a unit volume of oil under reservoir conditions was estimated at between $2,000 \text{ Nm}^3/\text{m}^3$ (minimum oil saturation – S_{or}) and $300 \text{ Nm}^3/\text{m}^3$ (maximum oil saturation – S_{wi}).

The highest value of final oil recovery through enriched gas injection was obtained under irreducible water saturation conditions.

Finally, as one would expect, comparison of the results of the oil displacement tests by water and by enriched gas, carried out under S_{wi} rock conditions, shows that enriched gas injection was more efficient than water injection in terms of the "microscopic displacement efficiency". In fact, oil recovery for enriched gas injection reached 99% against about 80% (maximum) for water-flooding.

ACKNOWLEDGEMENTS

The authors thank the management of Agip Oil, Libyan Branch, and ENI (Agip Division) for their permission to publish this paper. They extend their appreciation to all the colleagues at the Corporate E&P Laboratories who contributed to this work.

REFERENCES

- [1] Erba, M. *et al.*, 1983. Bu Attiffel Field – A synergistic geological and engineering approach to reservoir management, paper PD6 presented at 11th World Petroleum Congress, London.
- [2] Safsaf, S.R. and Michelotti, G., 1985 (April 16-18). Improved oil recovery by water flooding in Libyan oil fields operated by Agip (N.A.M.E.) Libyan Branch, paper presented at 3rd European Symposium on IOR, Rome.
- [3] Causin, E., Radaelli, F., Terzi, L. and El-Ageli, I.S., 1997 (October 20-22). Bu Attiffel field (Libya): Gas Injection Project – laboratory approach, paper EAGE 038 presented at 9th European Symposium on Improved Oil Recovery, The Hague, Netherlands.

[4] Yellig, W.F. and Metcalfe, R.S., 1980. Determination and prediction of CO_2 minimum miscibility pressure, *JPT*, 160-68.

[5] Godbole, S. P., Thele, K. J., and Reinbold, E. W., 1992 (October 4-7). EOS modeling and experimental observation of three-hydrocarbon-phase equilibria, paper SPE 24936 presented at 67th Annual Technical Conference and Exhibition, Washington.

[6] Zick, A. A., 1986. A combined condensing/vaporizing mechanism in the displacement of oil by enriched gas, paper SPE 15493, presented at 61st Annual Technical Conference and Exhibition, New Orleans, LA.

[7] Chierici, G. L., 1994. *Principles of Petroleum Reservoir Engineering -2*, Springer-Verlag.

[8] Causin, E. and Rossi, E., 1995 (15-20 June). Relative permeability at reservoir conditions, paper presented at THERMIE Workshop on IOR and EOR Technology in Europe, Beijing and Urumqi, China.

[9] Mohanty, K. K. and Miller, A. E., 1991 (September). Factor influencing unsteady state permeability of a mixed-wet reservoir rock, *SPEFE*, 349-358.

[10] Schechter, D. S. *et al.*, 1994. Low IFT drainage and imbibition, *J. Petr. Science and Eng.*, 283-300.

[11] Andreas, J. M. *et al.*, 1938. Boundary tension by pendant drop. *J. Phys. Chem.*, 1001.

[12] Hansen, F. K. and Rodshrud, G., 1991 (January). Surface tension by pendant drop. I. A fast standard instrument using computer image analysis. *J. Coll. Int. Sci.*

[13] Watson, A. T., *et al.*, 1988 (August). A regression-based method for estimating relative permeabilities from displacement experiment, *SPERE*, 953-958.